ROYAL SOCIETY OF CHEMISTRY

PAPER

Check for updates

Design of J-aggregates-like oligomers built from squaraine dyes exhibiting transparency in the visible regime and high fluorescence quantum yield in the NIR region†

Margarita Bužančić Milosavljević [ID] [a] and Vlasta Bonačić-Koutecký [ID] *[abc]

New materials for transparent luminescent solar concentrators (TLSCs) are of large interest. Therefore, we investigated the optical properties of J-aggregates-like oligomers (hereinafter referred to as J-aggregates) based on covalently bound squaraine dyes in toluene solvent using DFT and TD-DFT methods. In addition, the rate constants needed for the prediction of fluorescence quantum yield (QY) have been calculated using Fermi's Golden rule and vertical harmonic approximation (VH) for ground and excited states. In the context of QY prediction, different broadening of the lineshape has also been employed. We found that J-aggregates based on squaraine dyes exhibit near-infrared (NIR) selective absorption and emission as well as high fluorescence QY. Comparison of the properties obtained for dimers, trimers and tetramers belonging to two classes (SQA and SQB) of J-aggregates allows us to select the tetramer of SQA J-aggregates as suitable for application. The scaling model for $N \geq 4$ monomer subunits supports quantitative findings. Therefore, we propose J-aggregates containing $N \geq 4$ subunits of SQA with a central squaric acid ring with two oxygen atoms in toluene solvent as a suitable candidate for TLSC application.

1 Introduction

The design of materials with properties suitable for transparent luminescent solar concentrators (TLSCs) is a challenging task. TLSCs contain a harvesting surface with luminophores that should absorb and emit mainly outside the visible (VIS) region.[1–4] Adequate materials for such devices require high aesthetic quality and high power conversion efficiency,[5] which can be realized through transparency and by tuning optical efficiency. For this purpose, luminophores that harvest the ultraviolet (UV) and near-infrared (NIR) parts of the solar spectrum[6,7] and at the same time have high fluorescence quantum yield (QY)[5,8] are needed. For TLSC applications, the photophysical properties of luminophores, such as energy losses, have to be also considered. Among different luminophore energy losses, the reabsorption of photons seems to be

the important issue.[9] The minimization of the reabsorption loss can be achieved with lowering of the non-radiative decay processes and consequently enhancing the QY.[10–13] In the context of transparency and QY, some aggregates[14,15] have been studied.

In this contribution, we investigate J-aggregates based on covalently bound squaraine dyes as candidates fulfilling both conditions of transparency and high QY. Numerous applications of squaraine dyes have been accomplished, including their use in photovoltaic devices.[16,17] They have also been studied in the context of both high QY and NIR optical properties.[18–20] Experimental and theoretical work has been performed on J-aggregates built from squaraine dimers and trimers[21–23] to gain insight into their structural, optical, and exciton properties. In addition, the influence of oligomer chain length on optical characteristics has been investigated.[24–27] Recently, a review on luminescent solar concentrators (LSCs) gave a critical view of the field and its potential for the future.[28]

Squaraine based J-aggregates with a given number N of subunits producing a high QY can serve as UV and NIR selective harvesting materials. Therefore, they might be good candidates for integration into greenhouses, mobile electronics, and electric automobiles.

Fluorescence QY is determined by the ratio of the radiative rate k_r to the sum of the radiative rate k_r and all other non-

[a] Center of Excellence for Science and Technology-Integration of Mediterranean region (STIM), Faculty of Science, University of Split, Ruđera Boškovića 33, 21000 Split, Croatia. E-mail: margarita@stim.unist.hr

[b] Interdisciplinary Center for Advanced Science and Technology (ICAST) at University of Split, Meštrovićevo šetalište 45, 21000 Split, Croatia

[c] Department of Chemistry, Humboldt Universität zu Berlin, Brook-Taylor-Strasse 2, 12489 Berlin, Germany. E-mail: vbk@cms.hu-berlin.de

† Electronic supplementary information (ESI) available. See DOI: https://doi.org/10.1039/d3cp05291e

1314 | *Phys. Chem. Chem. Phys.*, 2024, **26**, 1314–1321

This journal is © the Owner Societies 2024

radiative decay rates $k_{nr} = k_{ic} + k_{isc}$ including internal conversion (IC) and intersystem crossing (ISC). A high value of QY can be obtained by increasing k_r and decreasing k_{nr} rates. This is particularly difficult to achieve in NIR since k_{ic} increases strongly with the reduction of the excitation energy. Since the optimization of a single chromophore in order to reach a high QY depends on many parameters, J-aggregates might be a simple alternative. The enhancement of the fluorescence QY in some J-aggregates has been assigned to superradiance due to the linear growth of the radiative rate with the delocalization length. Furthermore, the internal conversion rate k_{ic} simultaneously decreases with delocalization length. Both effects depend on the delocalization of excitons.[29]

In this contribution, in addition to optical properties, we present theoretical results for the QY prediction of SQA and SQB indolenine squaraine dyes in toluene solvent packed in J-aggregates. SQA contains a central squaric acid ring with two oxygen atoms as subunits and SQB squaraine dyes are formed by the dicyanovinylene group substitution at the central squaraine ring (*cf.* Scheme 1). For both J-aggregates built from SQA and SQB in toluene solvent, we investigated the optical properties in the VIS, UV, and NIR regimes in the context of application as materials for TLSC. Comparison of the theoretical and experimental optical properties of J-aggregates built from squaraine dimers and trimers serves to estimate the reliability of theoretical predictions. The results on the optical properties for tetramers of J-aggregates built from SQA and SQB squaraine dyes in toluene solvent, as well as QY values, serve to initiate additional experiments.

In order to determine the general trend of the internal conversion rate k_{ic} with the size N of the SQA and SQB J-aggregates, we use the scaling relation[29] based on the Englman and Jortner energy gap law.[30] This qualitative approach predicts lower k_{ic} and consequently higher QY values for SQA than for SQB J-aggregates. Although the SQB J-aggregates for $N \leq 4$ have QY values above 50%, higher QY values are preferable in the context of applications. In addition, minimized reabsorption loss can be achieved. We define the theoretical limit for intensity above 1.0 f_e as semitransparency in the VIS region of the absorption spectrum.

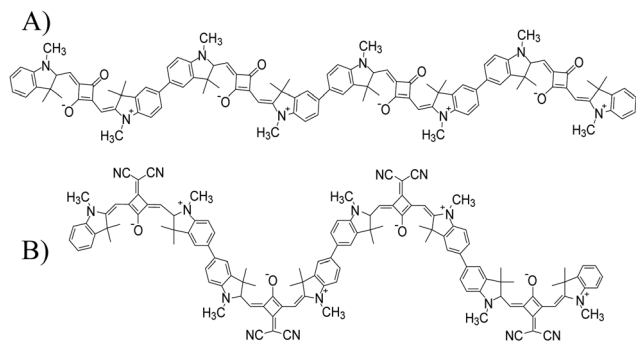Altogether, both conditions, such as transparency in the visible regime as well as absorption and emission in NIR with high fluorescence QY can be satisfied for SQA J-aggregates with $N \geq 4$. Therefore, we propose J-aggregates formed by SQA tetramers or by a larger number of subunits as new materials suitable for TLSC application.

2 Computational

Calculations of structural and optical properties, including the absorption and emission of J-aggregates in a solvent are necessary before determining radiative k_r and internal conversion rate k_{ic} constants needed for the calculation of fluorescence QY. For this purpose, we use density functional theory (DFT) for the optimization of molecular structures and time-dependent density functional theory (TD-DFT) to determine excited state properties using the Gaussian16[31] program. In both cases, the PBE0 hybrid functional[32,33] and def2-SVP[34] basis set are employed since they provide acceptable agreement with available experimental data. A comparison of the absorption spectra obtained by larger basis sets shows that the def2-SVP with 1230 AOs is adequate since the absorption spectra are not dependent on the choice of the tested basis sets (cc-pVTZ with 2628 AOs and def2-TZVP with 3050 AOs). The influence of different functionals on the absorption spectra has also been investigated. Comparison between experimental data for the most intense transition of the absorption spectrum for the trimer SQA J-aggregate shows the largest difference for CAM-B3LYP and wB97XD ($\sim$100 nm) and a smaller difference for B3LYP (30 nm) and PBE0 (63 nm) functionals. This supports the choice of either PBE0 or B3LYP functionals. The solvent effect has been included implicitly *via* the polarizable continuum model (PCM),[35] where excited state properties are calculated with equilibrium solvation (*cf.* ref. 36). For J-aggregates we use toluene solvent. Notice that optimization of structures for J-aggregates in toluene solvent has been carried out without symmetry constraints. If structural symmetry is present it has been introduced for the calculation of spectral properties.

Computational programs have been developed for the prediction of radiative k_r and non-radiative k_{nr} rates based on Fermi's Golden rule and harmonic approximation for ground and excited states.[37,38] In this contribution, we employ the FCclasses3 code to simulate vibrationally resolved fluorescence spectra and to determine the rate constants needed for the calculation of QY values (version FCclasses3-0.1,2019.[38]). Prediction of fluorescence quantum yields for molecules in solution remains a challenging task due to the harmonic approximation and the choice of line shape function. The used approximations have been previously critically addressed in the context of reliable rate prediction.[36]

Molecular potential energy surfaces (PES) are in principle not harmonic and therefore, the choice of the point at which the quadratic approximation is made defines different harmonic models. The models can be separated into two classes depending on around which point the PES of the electronic ground state is expanded to the second order. In the adiabatic hessian (AH) model the potential is expanded around the

Scheme 1 Structures of J-aggregates forming tetramers: (A) tetSQA and (B) tetSQB.

This journal is © the Owner Societies 2024

Phys. Chem. Chem. Phys., 2024, **26**, 1314–1321 | **1315**

geometry of the ground state minimum and excited state minimum, respectively. In the vertical hessian (VH) model the expansion occurs around the excited state minimum for both states. AH and VH models differ in equilibrium geometry and Hessian matrix.[39,40] They are the best models and should provide equal results if the harmonic approximation is valid. However, the AH model where two electronic states are described around different minimum energy structures (ground and excited) is not appropriate in the presence of large structural displacements. In this case, the VH model is recommended. Notice that for the VH model, the internal curvilinear coordinates better describe low-frequency modes than Cartesian coordinates, which can be responsible for the appearance of imaginary frequencies.[41] For calculations of semi-rigid molecules as J-aggregates, we use the VH model with internal curvilinear coordinates, as implemented in the FCclasses3 code and compare the results with experimental data. We have chosen temperature T = 300 K for the calculation of QY.

The broadening of the lineshape is also an important issue because of its different origins. The inhomogeneous broadening (Gaussian lineshape) is due to the fact that the environment acts differently on different molecules in solution. Therefore, it causes small shifts in energy levels, which in the ensemble of molecules form a Gaussian distribution that can be related to the thermal energy and the solvent reorganization energy.[42,43] The effect of inhomogeneous broadening on k_r and k_{ic} is usually small. Homogeneous broadening corresponding to the Lorentzian lineshape is a consequence of Heisenberg's uncertainty principle. Both types of broadening are combined in the Voigt profile. We use Voigt I and Voigt II, where the contribution of Lorentzian lineshape is an order of magnitude higher in Voigt I. The effect of Lorentzian broadening is negligible for k_r. In contrast, it influences substantially k_{ic}. The reliability of the predictions based on the first principle approach is not easy to judge. Therefore comparison with experimental results is useful. Nevertheless, due to the superradiant properties of J-aggregates, the trend of QY prediction is of interest in the context of applications and should be considered qualitatively. The influence of different broadening has been extensively investigated in ref. 36 and we consider the choice of broadening as a phenomenological parameter. For Gaussian broadening the choice of HWHM$_G$ = 0.02 eV reproduces well the experimental lineshape (cf. Fig. 1). Even if Lorentzian broadening can be estimated from the lifetime of the state $1/\tau$, it yields 4×10^{-5} eV (for dSQA) which in combination with Gaussian broadening (0.02 eV) within Voigt, does not influence the rates. Therefore, we use Lorentzian broadening as a parameter for checking reliability; if the k_{ic} dependence on broadening is large, the prediction is not reliable.[36]

Concerning charge transfer and transition dipole moments of studied J-aggregates, Fig. S1 and S2 (ESI†) confirm previous findings.[21–23,25–27] In addition, Fig. S1 (ESI†) also shows that the choice of functional, PBE0 versus CAM-B3LYP, does not influence the electron density difference (EDD) between the first excited state (S_1) and ground (S_0) states. The investigated
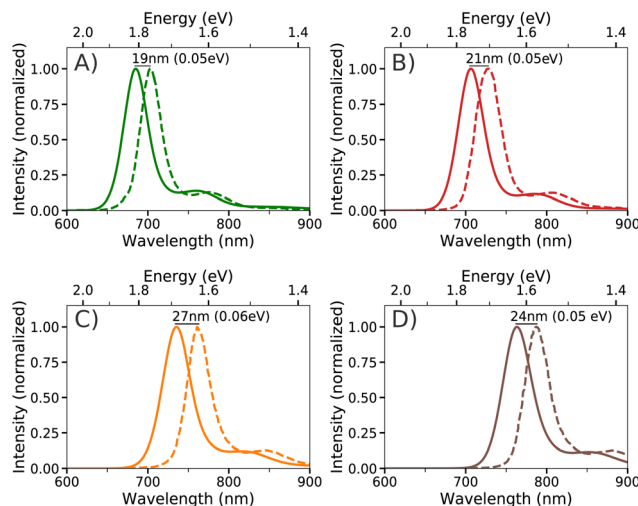

Fig. 1 Comparison between experimental (dashed line) and theoretical (full line) emission spectra for (A) dSQA, (B) tSQA, (C) dSQB, and (D) tSQB in toluene solvent. Theoretical emission spectra are obtained within the vertical hessian (VH) model using Gaussian broadening (HWHM$_G$ = 0.02), at 300 K. Experimental spectra were digitized from ref. 21.

squaraine J-aggregates exhibit linear structures (cf. Fig. 2) with localized transition dipole moments, which are arranged head-to-tail having out-of-phase orientation. The calculated electron density difference (cf. Fig. S1, ESI†) illustrates exciton nature according to Kasha's molecular exciton model.[44] Fig. S2 (ESI†) shows the enlargement of the dipole strength (μ^2) as the number of subunits increases, with higher values for SQA than SQB J-aggregates. With an increasing number of subunits in the J-aggregates, a superposition of the transition dipole moments causes a bathochromic shift and an increase in the intensity of the first excited state. These results agree with characteristics of absorption spectra of dimers, trimers and tetramers as shown in the Results and discussion (cf. Fig. 2, Fig. S3 and S4, ESI†).

In order to determine the qualitative trend of k_{ic} values as a function of the number of subunits N of the J-aggregate, we use the scaling relation (cf. Table S2 and eqn (S1) and (S2), ESI†) for SQA and SQB. For this purpose, the required parameters are taken from Table S2 (ESI†). These parameters are determined from DFT and TD-DFT calculations of SQA and SQB monomers in toluene solvent, while exciton coupling is calculated from Davydov splitting. The same functional and AO basis set have been used as for the calculation of structural and optical properties. For J-aggregates with weak exciton coupling,[29] the scaling relation yields a decrease of k_{ic} rate with the length N. This result together with the superradiative effect of J-aggregates is responsible for the high QY.

3 Results and discussion

The aim is to find J-aggregates built from squaraine dyes suitable for TLSC application. Therefore, we first address theoretically obtained optical properties of SQA and SQB dimers and trimers forming J-aggregates in toluene solvent
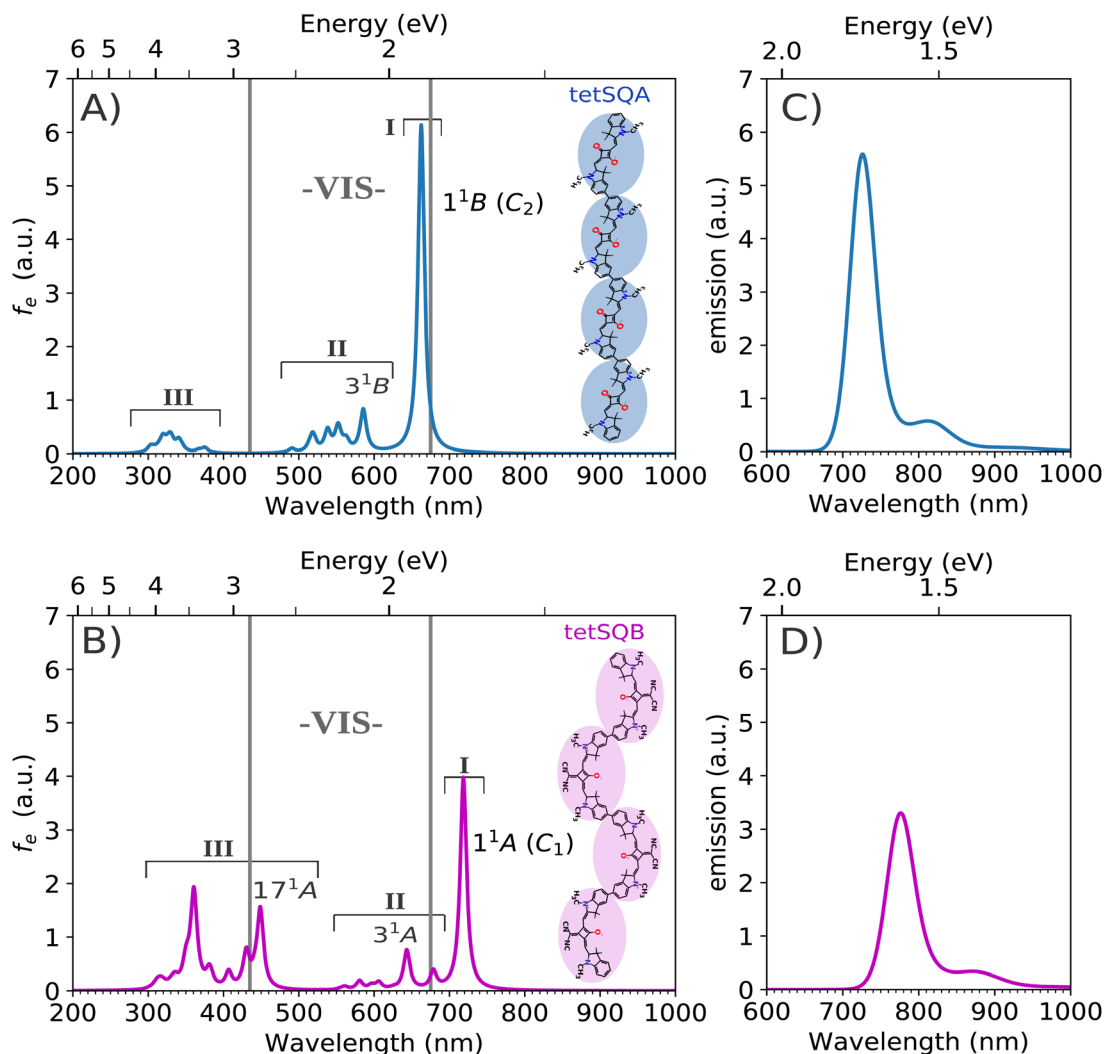
1316 | *Phys. Chem. Chem. Phys.*, 2024, **26**, 1314–1321

This journal is © the Owner Societies 2024

Fig. 2 TD-DFT absorption spectra of J-aggregates forming tetramers in toluene solvent: (A) tetSQA (blue) built from squaraine dyes with the central squaric acid ring and oxygen atoms, and (B) tetSQB (violet) built from squaraine dyes with the central squaric acid ring substituted with the dicyanovinylene group. The transitions are divided into groups I, II, and III. The most intense transitions (I) are labeled according to symmetry point groups. f_e labels oscillator strengths. The visible regime (VIS) is shown within gray lines. HOMO–LUMO gaps are 2.26 eV for tetSQA and 2.12 eV for tetSQB J-aggregates. Comparison between emission spectra of (C) tetSQA and (D) tetSQB J-aggregates in toluene solvent (*cf.* Computational). Notice that monomer subunits forming J-aggregates are covalently bound (1.5 Å).

for which experimental data[21] are available. They have been already investigated in different contexts.[22,23] Our calculated absorption and emission spectra for dimers (dSQA; dSQB) and trimers (tSQA; tSQB) are shown in Fig. S3 and S4 (ESI†). There are three groups of excited states (I, II, and III) present in the absorption spectra. Transitions due to HOMO–LUMO excitation with dominant intensities belong to group I, while groups II and III contain transitions with almost negligible intensities within the VIS and UV regimes, respectively. In order to obtain transparency for luminophores, the most intense transitions should be outside the VIS regime (435–675 nm[2]).

In the case of the dSQA, the calculated absorption spectrum in toluene solvent consists of two transitions characteristic of the J-aggregate peak splitting. The state 1^1B with the highest intensity is located at 625 nm (1.98 eV, group I), and the 4^1B state with very low intensity at 525 nm (2.36 eV, group II). They

correspond to the experimental ones measured at 690 nm (1.80 eV) and 621 nm (2.00 eV). States within the UV region (group III) have almost zero intensities (*cf.* Fig. S3A, ESI†). The dSQB spectrum is red shifted with respect to dSQA by 56 nm (*cf.* Table S1, ESI†). The most intense transition within group I lies outside the VIS regime and the transition 5^1A with very low intensity (group III) enters the VIS region (*cf.* Fig. S3B, ESI†). The difference between experimental and theoretical results is acceptable (*cf.* Computational).

The structure of the trimer tSQA has an inversion center and the absorption spectrum is characterized by two groups I and II belonging to J-aggregate features, which are also found experimentally (at 714 nm (1.74 eV) and 621 nm (2.00 eV)). They correspond to theoretically predicted 1^1A_u (at 652 nm (1.90 eV)) and 4^1A_u (at 563 nm (2.20 eV)) states as shown in Fig. S4A (ESI†). Group III does not contain any intense transitions. All

This journal is © the Owner Societies 2024

Phys. Chem. Chem. Phys., 2024, **26**, 1314–1321 | **1317**

three groups of transitions for the tSQB J-aggregate are shifted to lower energies with respect to those of tSQA. Therefore, the 10^1A peak of tSQB (group III) is entering the VIS regime and the most intense transition (group I) is in the NIR (*cf.* Fig. S4B, ESI†). Comparison between absorption spectra of dimers and trimers confirms the characteristic bathochromic shift that J-aggregates exhibit with an increasing number of monomers. The calculated properties of SQA and SQB monomers including absorption and emission spectra as well as k_{ic} rates, shown in Fig. S5 and S6 (ESI†), are in qualitative agreement with the measured ones.[21]

The fluorescence spectra obtained from the calculations of dimers and trimers demonstrate analog features as their equivalent absorption spectra. Their characteristic is a narrow emission J-band whose maximum is located in the NIR region. The difference between normalized theoretical emission spectra calculated within the vertical hessian model (VH) and experimental ones for dimers and trimers of J-aggregates in toluene solvent is not larger than 27 nm (*cf.* Fig. 1). In addition, the lineshapes of the theoretical and experimental emission spectra are very similar (*cf.* Fig. 1) justifying the use of the VH model. Notice that in comparison with measured spectra the calculated absorption and emission spectra for dimers and trimers of J-aggregates are always blue shifted by 62–66 nm (*cf.* Table S1, ESI†) and by 19–27 nm (*cf.* Fig. 1), respectively. For these J-aggregates, the experimental data[21] are in qualitative agreement with calculated properties.

Altogether, the described examples show the difference in absorption spectra between SQA and SQB of J-aggregates built from squaraine dyes. The increase in the number of subunits from dimers to trimers causes a red shift of absorption and emission. In addition, the qualitative agreement between theory and experiment for dimers and trimers motivated us to investigate J-aggregates containing tetramers as materials with suitable properties for applications.

Therefore, we present a comparison between theoretical absorption and emission spectra of tetramers tetSQA and tetSQB forming J-aggregates in toluene shown in Fig. 2. These results illustrate the influence of substitution at the central squaric acid ring by the dicyanovinylene group (tetSQB), but also show the red shift of the absorption due to increased size. Both tetSQA and tetSQB exhibit peak splitting within groups I and II following the J-aggregate features. Due to system elongation by one subunit, with respect to the SQA and SQB trimers, the calculated absorption spectra of the investigated tetramers are red shifted by 10 to 12 nm (*cf.* Table S1, ESI†). In addition to finding that the tetSQB state 1^1A is at 719 nm (1.72 eV), the location of the 1^1B state at 662 nm (1.87 eV) for the tetSQA J-aggregate is reaching the NIR region. In spite of the blue shift emerging from theoretical calculations due to the choice of DFT functional, the state with the largest intensity in the NIR region is present for both tetramers. The transparent visible regime of tetSQA contains low intensity states belonging to groups II and III located at 491–586 nm (2.53–2.12 eV) and 303–375 nm (4.09–3.31 eV), respectively. This is also valid for tetSQB transitions at 555–679 nm (2.23–1.83 eV) within group II.

In contrast, due to the state 17^1A in the VIS regime (at 449 nm (2.76 eV)) the transition intensities of tetSQB within group III are not negligible, therefore representing semitransparency. According to the above spectral analysis, the tetSQA J-aggregate fulfills the transparency requirements. The tetSQB NIR shift is in agreement with the smaller HOMO–LUMO gap in comparison with the tetSQA (*cf.* caption of Fig. 2). The emission spectra of both tetramers are in the red regime but tetSQA has a larger intensity for emission and absorption spectra than tetSQB. In addition, the shape of the absorption and emission spectra is important in the context of reabsorption loss. Notice that there is no significant overlap between absorption and emission spectra since the absorption spectral tail is characterized by the sharp edge and the emission spectra have a narrow shape. This is convenient because the small overlap can minimize the reabsorption loss by lowering the non-radiative rate and enhancing the QY value.

The calculated radiative k_r and internal conversion rate k_{ic} in toluene solvent for dimers, trimers and tetramers of J-aggregates together with the fluorescence QY, obtained using the FCclasses code, are presented in Table 1. The most challenging aspect of k_{ic} rate prediction is the choice of the broadening function. The predicted values strongly depend on details of the simulated emission spectrum (*cf.* Fig. 1). As described in ref. 36 the predicted value of k_{ic} has to be critically considered. Since k_{ic} depends on the description of highly excited vibronic states which are responsible for the very far tail of the emission spectra, they are only approximately described by different

Table 1 Fluorescence quantum yields QY = $k_r/(k_r + k_{ic})$ of J-aggregates calculated within the vertical hessian model (VH) in toluene solvent (at 300 K) using the FCclasses3 program (version FCclasses3-0.1,2019.[38]). The broadening functions are Gaussian (HWHM$_G$ = 0.02 eV), Voigt I (HWHM$_G$ = 0.02 eV, HWHM$_L$ = 0.001 eV) and Voigt II (HWHM$_G$ = 0.02 eV, HWHM$_L$ = 0.0001 eV). k_{nr} labels the experimental non-radiative rate

Squaraine	Broad. f.	k_r (10^8 s^{-1}) VH	Exp.	k_{ic} (s^{-1}) VH	k_{nr} (s^{-1}) Exp.	QY VH	Exp.[21]
dSQA	Voigt I	4.1	4.9	3.2×10^8	1.1×10^8	0.56	0.82
	Voigt II	4.2		1.2×10^8		0.77	
	Gauss	4.2		1.0×10^8		0.80	
dSQB	Voigt I	2.6	2.7	2.7×10^8	1.2×10^8	0.49	0.69
	Voigt II	2.6		4.6×10^7		0.85	
	Gauss	2.6		2.2×10^7		0.92	
tSQA	Voigt I	5.4	5.4	2.3×10^8	9.6×10^7	0.70	0.85
	Voigt II	5.6		2.4×10^7		0.96	
	Gauss	5.6		1.7×10^6		1.00	
tSQB	Voigt I	3.0	2.8	2.7×10^8	2.1×10^8	0.53	0.58
	Voigt II	3.1		2.9×10^7		0.92	
	Gauss	3.2		1.8×10^6		0.99	
tetSQA	Voigt I	6.5		2.6×10^8		0.71	
	Voigt II	6.7		3.5×10^7		0.95	
	Gauss	6.7		9.2×10^6		0.99	
tetSQB	Voigt I	3.7		3.6×10^8		0.51	
	Voigt II	3.9		9.1×10^7		0.81	
	Gauss	3.9		6.1×10^7		0.87	

1318 | *Phys. Chem. Chem. Phys.*, 2024, **26**, 1314–1321
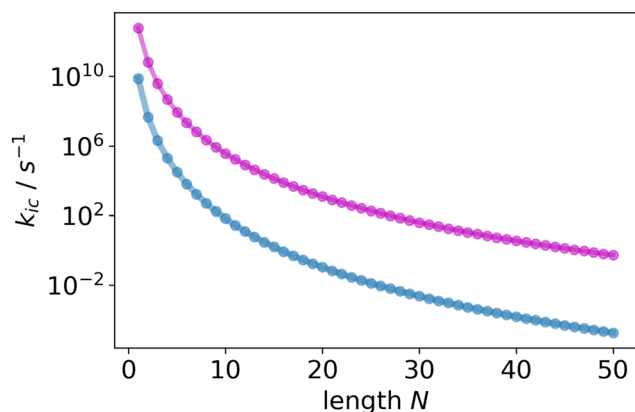
This journal is © the Owner Societies 2024

Fig. 3 Scaling of k_{ic} rate with length N of SQA (blue) and SQB (violet) J-aggregates. Parameters for scaling are determined from TD-DFT calculations of SQA and SQB (*cf.* Scaling relations and Table S2 in the ESI†). Comparison of k_{ic} values for SQA/SQB as a function of N subunits: $7.9 \times 10^9/6.1 \times 10^{12}$ for $N = 1$; $4.6 \times 10^7/6.5 \times 10^{10}$ for $N = 2$; $2.1 \times 10^6/3.9 \times 10^9$ for $N = 3$; $2.0 \times 10^5/4.8 \times 10^8$ for $N = 4$; and $3.1 \times 10^4/8.8 \times 10^7$ for $N = 5$.

broadenings. For example, a broad emission spectrum is connected with large k_{ic}. The influence of broadening on k_{ic} values has been illustrated in Table 1 on examples of Voigt I, Voigt II and Gaussian lineshapes (*cf.* Computational). Voigt I provides the closest results of k_{ic} to the available experimental one. The k_r values are independent from broadening and correlate very well with measurements for investigated dimers and trimers (*cf.* Table 1). In both cases, experimentally and theoretically, there is a clear superradiance effect observed, with enlargement of the k_r rate with the system size including the tetramers. This increase of radiative rate is experimentally much less pronounced for dSQB and tSQB with respect to the dSQA and tSQA.

The experimental k_{ic} rates for dimers and trimers decrease for SQA and increase for SQB. The calculated k_{ic} rates for SQA J-aggregates decrease also from dimer to trimer and in the case of tetSQA, the k_{ic} value is smaller than for dSQA. This produces an increase of QY (0.56–0.71, Voigt I) with system size. The QY values for the SQA dimer and trimer in toluene are in acceptable agreement with experimentally measured values, which are larger than 80%. In the case of SQB J-aggregates the theoretically predicted k_{ic} follows the experimental trend: the dimer and trimer have the same value for k_{ic} which increases for the tetramer. However, together with the enlargement of k_r, similar values for theoretically predicted QY for SQB J-aggregates have been obtained, including a very small decrease from trimer to tetramer (0.53–0.51, Voigt I).

The dSQB and tSQB have lower QY values in toluene solvent than dSQA and tSQA. Notice that the polarity of the solvent can strongly influence the values of QY. Therefore lower QY values for J-aggregates built from SQB in a polar solvent[26] (trichloromethane) than in non-polar solvent[21] (toluene) are to be expected. In addition, dSQB and tSQB are more dependent on broadening. In the case of Voigt I, the values of broadening are in agreement with the measured ones, which are lower than for SQA dimers and trimers. Furthermore, the theoretical value of quantum yield for tetSQA is larger than 70% and for tetSQB is

larger than 50%, as shown in Table 1. The influence of broadening on all calculated k_{ic} rates for SQA and SQB is shown in Fig. S7 (ESI†). In the case of tetSQA and tetSQB, the broadening does not influence substantially the k_{ic} values allowing us to accept the prediction that QY is lower for tetSQB than for tetSQA. Therefore, the SQA tetramer satisfies both conditions, transparency and high QY. In order to extend the QY predictions for systems with subunits $N \geq 4$, we present a comparison of k_{ic} rate constants for the SQA and SQB J-aggregates using the scaling factor relation[29] in Fig. 3 (for very approximate qualitative scaling relation *cf.* ESI†). Both k_{ic} rates decrease with N, but k_{ic} for SQA J-aggregates is considerably lower than k_{ic} for SQB J-aggregates under the assumption of weak exciton coupling J_{ge} for SQA and SQB (-881 cm^{-1} and -645 cm^{-1}) defined in ref. 29. The qualitative approach supports our computational results also for tetramers. This means that the values of QY are larger for SQA than for SQB J-aggregates. In summary, according to the described findings and in order to initiate new experiments, we propose SQA J-aggregates with subunits ≥ 4 as suitable materials for TLSC applications.

4 Conclusions

Our theoretical study of optical properties as well as prediction of QY for SQA and SQB squaraine-based J-aggregates in toluene solvent provided us with the following results:

(i) Increasing number of subunits in J-aggregates is responsible for the red shift and intensity enhancement of the absorption and emission spectra.

(ii) Characteristics of J-aggregate's spectral properties containing one dominantly intense state and several states with very low intensities are present for all investigated cases.

(iii) The main findings in the context of TLSC application are the difference between SQA and SQB J-aggregates for the given number of subunits. This includes both the presence of absorption and emission states with large intensities outside the VIS regime and high fluorescence QY.

(iv) In the case of SQA dimers and trimers, the estimated computational error for the most intense transition is 62–66 nm. Therefore, the most intense transition is within the NIR regime.

(v) The SQA tetramer shows the dominant state in the NIR regime based on theoretical predictions including estimated computational error (*cf.* iv).

(vi) The calculated QY for SQA is larger than for SQB. These findings are also supported by a qualitative approach based on the scaling model.

Altogether tetSQA squaraine J-aggregate in toluene solvent or SQA J-aggregates with a larger numbers of subunits seem to be appropriate materials for TLSC application.

Conflicts of interest

There are no conflicts to declare.

This journal is © the Owner Societies 2024

Phys. Chem. Chem. Phys., 2024, **26**, 1314–1321 | **1319**

Acknowledgements

References

1 M. Currie, T. Heidel, S. Goffri and M. Baldo, *Science*, 2008, **321**, 226–228.

2 R. R. Lunt, *Appl. Phys. Lett.*, 2012, **101**, 043902.

3 Y. Zhao, G. A. Meek, B. G. Levine and R. R. Lunt, *Adv. Opt. Mater.*, 2014, **2**, 606–611.

4 C. Yang and R. R. Lunt, *Adv. Opt. Mater.*, 2017, **5**, 1600851.

5 C. Yang, D. Liu and R. R. Lunt, *Joule*, 2019, **3**, 2871–2876.

6 K. Zhang, C. Qin, X. Yang, A. Islam, S. Zhang, H. Chen and L. Han, *Adv. Energy Mater.*, 2014, **4**, 1301966.

7 C. Yang, W. Sheng, M. Moemeni, M. Bates, C. K. Herrera, B. Borhan and R. R. Lunt, *Adv. Energy Mater.*, 2021, **11**, 2003581.

8 Y. Zhao and R. R. Lunt, *Adv. Energy Mater.*, 2013, **3**, 1143–1148.

9 C. Yang, J. Zhang, W.-T. Peng, W. Sheng, D. Liu, P. Kuttipillai, M. Young, M. Donahue, B. Levine, B. Borhan and R. Lunt, *Sci. Rep.*, 2018, **8**, 16359.

10 M. G. Debije and P. P. C. Verbunt, *Adv. Energy Mater.*, 2012, **2**, 12–35.

11 J. L. Banal, B. Zhang, D. J. Jones, K. P. Ghiggino and W. W. H. Wong, *Acc. Chem. Res.*, 2017, **50**, 49–57.

12 F. Proise, A.-L. Joudrier, J.-L. Pelouard and J.-F. Guillemoles, *EPJ Photovoltaics*, 2018, **9**, 12.

13 B. Zhang, C. Gao, N. Neto and W. Wong, *Principles and Applications of Aggregation-Induced Emission*, 2019, pp. 479–504.

14 A. Eisfeld and J. S. Briggs, *Phys. Status Solidi A*, 2018, **215**, 1700634.

15 J. L. Banal, J. M. White, T. W. Lam, A. W. Blakers, K. P. Ghiggino and W. W. H. Wong, *Adv. Energy Mater.*, 2015, **5**, 1500818.

16 K. Ilina, W. M. MacCuaig, M. Laramie, J. N. Jeouty, L. R. McNally and M. Henary, *Bioconjugate Chem.*, 2020, **31**, 194–213.

17 J. He, Y. J. Jo, X. Sun, W. Qiao, J. Ok, T.-I. Kim and Z. Li, *Adv. Funct. Mater.*, 2020, **31**, 2008201.

18 L. E. McNamara, T. A. Rill, A. J. Huckaba, V. Ganeshraj, J. Gayton, R. A. Nelson, E. A. Sharpe, A. Dass, N. I. Hammer and J. H. Delcamp, *Chemistry*, 2017, **23**, 12494–12501.

19 A. Zampetti, A. Minotto and F. Cacialli, *Adv. Funct. Mater.*, 2019, **29**, 1807623.

20 K. Strassel, A. Kaiser, S. Jenatsch, A. C. Véron, S. B. Anantharaman, E. Hack, M. Diethelm, F. Nüesch, R. Aderne, C. Legnani, S. Yakunin, M. Cremona and R. Hany, *ACS Appl. Mater. Interfaces*, 2018, **10**, 11063–11069.

21 H. Ceymann, A. Rosspeintner, M. H. Schreck, C. Mützel, A. Stoy, E. Vauthey and C. Lambert, *Phys. Chem. Chem. Phys.*, 2016, **18**, 16404–16413.

22 M. I. S. Röhr, H. Marciniak, J. Hoche, M. H. Schreck, H. Ceymann, R. Mitric and C. Lambert, *J. Phys. Chem. C*, 2018, **122**, 8082–8093.

23 C. Heshmatpour, P. Malevich, F. Plasser, M. Menger, C. Lambert, F. Šanda and J. Hauer, *J. Phys. Chem. Lett.*, 2020, **11**, 7776–7781.

24 S. F. Völker, S. Uemura, M. Limpinsel, M. Mingebach, C. Deibel, V. Dyakonov and C. Lambert, *Macromol. Chem. Phys.*, 2010, **211**, 1098–1108.

25 C. Lambert, F. Koch, S. F. Völker, A. Schmiedel, M. Holzapfel, A. Humeniuk, M. I. S. Röhr, R. Mitric and T. Brixner, *J. Am. Chem. Soc.*, 2015, **137**, 7851–7861.

26 A. Turkin, P. Malý and C. Lambert, *Phys. Chem. Chem. Phys.*, 2021, **23**, 18393–18403.

27 J. Selby, M. Holzapfel, K. Radacki, A. K. Swain, H. Braunschweig and C. Lambert, *Macromolecules*, 2022, **55**, 421–436.

28 M. Cao, X. Zhao and X. Gong, *JACS Au*, 2023, **3**, 25–35.

29 A. Humeniuk, R. Mitrić and V. Bonačić-Koutecký, *J. Phys. Chem. A*, 2020, **124**, 10143–10151.

30 R. Englman and J. Jortner, *Mol. Phys.*, 1970, **18**, 145–164.

31 M. J. Frisch, G. W. Trucks, H. B. Schlegel, G. E. Scuseria, M. A. Robb, J. R. Cheeseman, G. Scalmani, V. Barone, G. A. Petersson, H. Nakatsuji, X. Li, M. Caricato, A. V. Marenich, J. Bloino, B. G. Janesko, R. Gomperts, B. Mennucci, H. P. Hratchian, J. V. Ortiz, A. F. Izmaylov, J. L. Sonnenberg, D. Williams-Young, F. Ding, F. Lipparini, F. Egidi, J. Goings, B. Peng, A. Petrone, T. Henderson, D. Ranasinghe, V. G. Zakrzewski, J. Gao, N. Rega, G. Zheng, W. Liang, M. Hada, M. Ehara, K. Toyota, R. Fukuda, J. Hasegawa, M. Ishida, T. Nakajima, Y. Honda, O. Kitao, H. Nakai, T. Vreven, K. Throssell, J. A. Montgomery, Jr., J. E. Peralta, F. Ogliaro, M. J. Bearpark, J. J. Heyd, E. N. Brothers, K. N. Kudin, V. N. Staroverov, T. A. Keith, R. Kobayashi, J. Normand, K. Raghavachari, A. P. Rendell, J. C. Burant, S. S. Iyengar, J. Tomasi, M. Cossi, J. M. Millam, M. Klene, C. Adamo, R. Cammi, J. W. Ochterski, R. L. Martin, K. Morokuma, O. Farkas, J. B. Foresman and D. J. Fox, *Gaussian 16 Revision A.03*, Gaussian Inc, Wallingford CT, 2016.

32 C. Adamo and V. Barone, *J. Chem. Phys.*, 1999, **110**, 6158–6170.

33 M. Ernzerhof and G. E. Scuseria, *J. Chem. Phys.*, 1999, **110**, 5029–5036.

34 F. Weigend, *Phys. Chem. Chem. Phys.*, 2006, **8**, 1057–1065.

35 J. Tomasi, B. Mennucci and R. Cammi, *Chem. Rev.*, 2005, **105**, 2999–3094.

36 A. Humeniuk, M. Bužančić, J. Hoche, J. Cerezo, R. Mitrić, F. Santoro and V. Bonačić-Koutecký, *J. Chem. Phys.*, 2020, **152**, 054107.

1320 | *Phys. Chem. Chem. Phys.*, 2024, **26**, 1314–1321

This journal is © the Owner Societies 2024

37 Y. Niu, W. Li, Q. Peng, H. Geng, Y. Yi, L. Wang, G. Nan, D. Wang and Z. Shuai, *Mol. Phys.*, 2018, **116**, 1078–1090.

38 F. Santoro and J. Cerezo, FCclasses3, a code to simulate electronic spectra. Version FCclasses3-0.1, 2019. Visit **https://www.pi.iccom.cnr.it/fcclasses**.

39 F. J. Avila Ferrer and F. Santoro, *Phys. Chem. Chem. Phys.*, 2012, **14**, 13549–13563.

40 F. Santoro and D. Jacquemin, *Wiley Interdiscip. Rev.: Comput. Mol. Sci.*, 2016, **6**, 460–486.

41 J. Cerezo and F. Santoro, *J. Chem. Theory Comput.*, 2016, **12**, 4970–4985.

42 R. Marcus, *J. Chem. Phys.*, 1965, **43**, 1261–1274.

43 F. J. A. Ferrer, R. Improta, F. Santoro and V. Barone, *Phys. Chem. Chem. Phys.*, 2011, **13**, 17007–17012.

44 M. Kasha, *Radiat. Res.*, 1963, **20**, 55–71.

This journal is © the Owner Societies 2024

Phys. Chem. Chem. Phys., 2024, **26**, 1314–1321 | **1321**